**Quantum dynamics of electron-transfer reactions: photoinduced intermolecular electron transfer in a porphyrin–quinone complex**

*Molecular Physics*
Vol. 00, No. 00, Month 200x, 1–26

## RESEARCH ARTICLE

# Quantum dynamics of electron-transfer reactions: Photoinduced intermolecular electron transfer in a porphyrin-quinone complex

Raffaele Borrelli[a*], Michael Thoss[b*], Haobin Wang[c], Wolfgang Domcke[d]

[a] *Dipartimento di Valorizzazione e Protezione delle Risorse Agroforestali, Università di Torino, I-84084 Grugliasco, Torino, Italy*; [b] *Institut für Theoretische Physik und Interdisziplinäres Zentrum für Molekulare Materialien, Friedrich-Alexander-Universität Erlangen-Nürnberg, Staudtstr. 7/B2, D-91058 Erlangen, Germany.*; [c] *Department of Chemistry and Biochemistry, MSC 3C, New Mexico State University, Las Cruces, NM 88003, USA.* [d] *Department of Chemistry, Technische Universität München, D-85748 Garching, Germany.*

(*Received 00 Month 200x; final version received 00 Month 200x*)

Photoinduced electron-transfer (ET) between a magnesium-porphyrin and benzoquinone in a model molecular complex is investigated employing *ab initio* multi-configuration electronic-structure calculations combined with quantum dynamical methods. The microscopic parameters controlling the electron-transfer process are obtained using a first-principles diabatization procedure. A model Hamiltonian which includes both linear and quadratic vibronic couplings of all nuclear degrees of freedom of the system is constructed. Quantum dynamical simulations of the ET process are performed employing the multilayer multiconfiguration time-dependent Hartree method. A detailed analysis of the ET dynamics for models of increasing complexity reveals that the dynamics is strongly influenced by resonances associated with vibronically active nuclear modes, leading to significant deviations from the results of classical ET theory. The comparison with results obtained with the simplified spin-boson model reveals the effects related to the Duschinsky rotation of normal modes.

*Corresponding authors: E-mail: raffaele.borrelli@unito.it
*E-mail: michael.thoss@physik.uni-erlangen.de

ISSN: 0040-5167 print/ISSN 1754-2278 online

DOI: 10.1080/0040516YYxxxxxxxx
http://www.informaworld.com

## 1. Introduction

Photoinduced electron-transfer (ET) reactions are the basic processes of solar energy conversion both in living systems and in artificial molecular machines.[1–4] In recent decades, a large variety of model systems have been experimentally investigated with the aim of understanding the detailed molecular mechanisms of such processes. Amongst others, supramolecular complexes consisting of porphyrin-type or phtalocyanine-type electron donors and quinone-type electron acceptors have been of interest, mainly as simplified models of the primary charge-separation process which takes place in biological systems. Understanding the mechanistic aspects of ET in such models is of great importance not only for scientific purposes, but also for technological progress, especially for the development of new devices capable of producing solar fuels, electric energy, and for the emerging field of molecular electronics. In particular, a better comprehension of the role played by intramolecular and intermolecular vibrations as well as by the solvent is essential. This requires the development and assessment of theoretical models based on a fully microscopic description of the electronic and nuclear properties of the electron donor-acceptor pair.

A standard model for studying ET processes in molecules is the spin-boson Hamiltonian.[5–7] The dynamics of this model has been characterized by numerically exact methods, providing much insight into the mechanisms of ET reactions.[8–16] While this model represents a cornerstone for treating the interaction of a microscopic system with a thermal bath, e.g. in outer-sphere electron transfer reactions, its application to describe the coupling of the internal vibrational degrees of freedom of a molecular system to an ET process can be questionable. In particular, the assumption that the shape of the potential energy surfaces is the same in both diabatic electronic states is quite stringent, and often not fulfilled in real systems.

As an example, we consider here photoinduced ET in a Mg-porphyrin-benzoquinone complex. In previous work, we have developed a model Hamiltonian to describe the photoinduced ET reaction in this system, which takes into account both the effects of the displacement of the equilibrium geometries and the variation of the normal modes upon ET (Duschinsky effect).[17] The structure of the complex is shown in figure 1.[17, 18] The overall system has $C_s$ symmetry and the minimum atom-atom distance is about 4.5 Å, whereas the center-to-center distance

of the two rings is about 6.5 Å. The motivation for this choice is to allow an easy extension of the present calculations to the more complex case of ET reactions coupled to water oxidation processes as described by Sobolewski and Domcke,[18] which will be the subject of future research. Indeed the system is derived from a partial optimization of a supramolecular complex in which a Mg-porphyrin is bridged by a water molecule to the quinone moiety, with subsequent removal of the water molecule. It is noted that albeit the arrangement of the donor-acceptor pair in the complex does influence the ET rate, most of the qualitative results presented in this paper remain valid for a large class of porphyrin-quinone complexes, independent of the mutual orientation and the distance of the two moieties.

Extending previous work on the basis of reduced dimensionality models of the ET complex,[17] we provide in this paper a detailed analysis of the dynamics of ET and its dependence on the driving force, employing the multilayer multiconfiguration time-dependent Hartree (ML-MCTDH) method. Using this approach, it is possible to provide an accurate treatment of the dynamics of the ET process including all 135 intramolecular vibrational degrees of freedom of the system. In this study, we focus on the effect of the intramolecular modes of the donor and acceptor moiety and neglect the influence of a possible surrounding medium as well as of low-frequency intermolecular motion. Previous works have shown that the application of such a model to study ET reactions in biological systems can provide a wealth of information on the relative importance of the different types of nuclear motion on the ET rates. [19–25]

This paper is structured as follows. In Sec. 2, we outline the theoretical methodology employed to study the photoinduced ET reaction in the Mg-porphyrin-benzoquinone complex. This includes the description of the model Hamiltonian, the details of the electronic structure calculations used to determine the parameters of the Hamiltonian, as well as a brief description of the ML-MCTDH method. The results of the simulations for the ET dynamics are discussed in Sec. III. Considering models of increasing complexity, the mechanisms of the ET reaction are analyzed, in particular the role of the vibrational degrees of freedom. Sec. IV concludes with a summary.

INSERT FIGURE 1

## 2. Methodology

### 2.1. *Model Hamiltonian for Porphyrin-Quinone ET*

ET in a weakly interacting donor-acceptor pair can conveniently be described as a transition between two diabatic electronic states, corresponding to reactants and products, respectively. In the case of an electron donor-acceptor pair, the diabatic states can be constructed as a product of the electronic states of the two non-interacting moieties. However, the actual implementation of such an intuitive definition faces a number of technical difficulties, and in most cases diabatic states are obtained as a unitary transformation of the adiabatic states. The numerical methodology used to derive the diabatic representation in this work is described in the next section.

The diabatic model Hamiltonian, $H$, employed here has the typical form:

$$H = \left|\mathrm{P^*Q}\right\rangle(T+U^e)\left\langle\mathrm{P^*Q}\right| + \left|\mathrm{P^+Q^-}\right\rangle(T+U^{\mathrm{ct}})\left\langle\mathrm{P^+Q^-}\right| + V\left|\mathrm{P^*Q}\right\rangle\left\langle\mathrm{P^+Q^-}\right| + c.c. \tag{1}$$

where $\left|\mathrm{P^*Q}\right\rangle$ denotes the locally-excited state of the complex, in which the porphyrin is in its first excited singlet state ($\mathrm{S_1}$) and the quinone in its ground state, $\left|\mathrm{P^+Q^-}\right\rangle$ is the charge-transfer state, $U^e$ and $U^{ct}$ are their respective potential-energy surfaces (PES), $T$ is the nuclear kinetic-energy operator, and $V$ the diabatic electronic coupling. As already pointed out, we neglect any intermolecular motion, and further assume that the PESs of the diabatic electronic states can be written as the sum of the PESs of the two separate molecules. Finally, the harmonic approximation is employed. Using the normal-mode representation, we can write the PESs of the two diabatic states as

$$U^e = \frac{1}{2}\sum_i \omega_{Pi} q_{Pi}^2 + \frac{1}{2}\sum_j \omega_{Qj} q_{Qj}^2 \tag{2}$$

$$U^{\mathrm{ct}} = \frac{1}{2}\sum_i \tilde{\omega}_{Pi} \tilde{q}_{Pi}^2 + \frac{1}{2}\sum_j \tilde{\omega}_{Qj} \tilde{q}_{Qj}^2 + \Delta E^\circ. \tag{3}$$

Here, $q_{Qj}, \omega_{Qi}$ denote the dimensionless coordinates of the vibrational normal modes and the frequencies of benzoquinone in its ground state, respectively, and $q_{Pi}, \omega_{Pi}$ those of porphyrin in is first excited state. Analogously, $\tilde{q}_{Qj}, \tilde{\omega}_{Qj}$, and $\tilde{q}_{Pi}, \tilde{\omega}_{Pi}$, are the vibrational normal modes and the corresponding frequencies of the benzoquinone radical anion, $\mathrm{Q^{\cdot -}}$, and of the porphyrin radical cation, $\mathrm{P^{\cdot +}}$,

respectively. $\Delta E^\circ$ denotes the driving force of the ET reaction.

For computational purposes it is often better to write the two PESs in terms of the same set of variables.[26] To this end, Duschinsky's transformation can be used to express the normal modes of the CT state in terms of those of the initial electronic state

$$\tilde{q}_P = J_P q_P + d_P, \qquad \tilde{q}_Q = J_Q q_Q + d_Q, \tag{4}$$

where the vectors $d_P, d_Q$ represent the displacements of the equilibrium positions of the normal modes of vibration upon ET, and the linear transformation matrices $J_P, J_Q$ (the so-called Duschinsky matrices) account for variations of directions and frequencies of normal modes. Then, by substituting equations (4) into equation (3), we obtain the transformed PES of the CT state

$$U^{\mathrm{ct}} = \Delta E_{\mathrm{v}} + \sum_{X=P,Q} \left\{ \sum_i \kappa_i^X q_{Xi} + \frac{1}{2} \sum_{i,j} \gamma_{ij}^X q_{Xi} q_{Xj} \right\} \tag{5}$$

where the linear vibronic couplings $\kappa_i^{\{P,Q\}}$, the Hessian $\gamma_{ij}^{\{P,Q\}}$, and the energy difference $\Delta E_v$ are defined as

$$\kappa_i^X = \tilde{\omega}_{Xi} \sum_j J_{Xij} d_{Xj} \tag{6}$$

$$\gamma_{ij}^X = \sum_k J_{Xik} \tilde{\omega}_{Xk} J_{Xkj}, \qquad X = P, Q \tag{7}$$

$$\Delta E_v = \Delta E^\circ + \lambda_Q + \lambda_P, \tag{8}$$

$\lambda_P, \lambda_Q$ being the reorganization energies of Mg-porphyrin and benzoquinone respectively, defined as

$$\lambda_P = \frac{1}{2} \sum_i d_{Pi}^2 \tilde{\omega}_{Pi}, \qquad \lambda_Q = \frac{1}{2} \sum_i d_{Qi}^2 \tilde{\omega}_{Qi}.$$

$\Delta E_v$ represents the vertical energy difference between two electronic states, *i.e.* computed at the equilibrium geometry of the electronic ground state. We notice that the linear vibronic terms depend on normal-modes shifts, and ultimately on the changes of the equilibrium geometries of the molecules upon ET. Second-order terms depend on the variation of the vibrational frequencies and on the mixing of normal modes, *i.e.* the Duschinsky effect. Neglecting off-diagonal second order terms and assuming that the vibrational frequencies remain unchanged upon ET,

a spin-boson type Hamiltonian is recovered.

Finally, the diabatic electronic coupling, $V$, is approximated to be independent of the nuclear coordinates (Condon approximation). This is an ubiquitous assumption in the theory of ET reactions, which can be safely applied here, since both the excited state and the CT state belong to the $A'$ symmetry representation, thus allowing for a purely electronic coupling term. The dependence of the coupling on the nuclear coordinates is an important issue which is rarely addressed due to its complexity. Recent studies suggest that in donor-acceptor systems connected by a rigid spacer the Condon approximation is a rather realistic model.[27] Details of the calculation of $V$ are given in the next section.

### 2.2. *Electronic-Structure Calculations*

The diabatic electronic states employed in the model Hamiltonian, Eq. (1), have been obtained using an *ab initio* quasi-diabatization procedure. In this procedure, the electronic eigenstates, $\{\Phi_i^\circ\}$, of the porphyrin-quinone pair at a very large distance (50 Å), *i.e.* with a vanishingly small interaction, are computed and taken as reference diabatic states. At such a distance the first excited state of the system corresponds to the CT state with an electron fully transferred to the quinone, and the second excited state corresponds to the locally excited state of the Mg-porphyrin. The CT state cannot be directly excited since it has a vanishing transition dipole. Then, the porphyrin-quinone intermolecular distance is changed to the value of interest, in our case 4.5 Å, and a new set, $\{\Phi_i\}$, of adiabatic electronic eigenstates is computed. Finally, diabatic states, $\{\Psi_i\}$, are obtained by a unitary transformation of the adiabatic states, $\{\Phi_i\}$. The unitary transformation is determined by maximizing the overlap, $\langle\Psi_i|\Phi_i^\circ\rangle$, between the diabatic wavefunctions and the reference states. The technique used for the overlap maximization is described in detail in refs. [28] and [29] and is implemented in the Molpro software.[30] Once the unitary transformation is determined, the adiabatic electronic Hamiltonian can be easily transformed to the diabatic Hamiltonian, providing the energies and the diabatic coupling matrix element which is responsible for the ET process.

The electronic states have been obtained using a state-averaged multi-configuration self-consistent field (SA-MCSCF) method, with the standard Dunning cc-pVTZ basis set.[31] The active space of the MCSCF calculations includes six orbitals localized on the Mg-porphyrin and three orbitals localized on the benzoquinone. The results of the MCSCF calculations show that the Mg-porphyrin-

benzoquinone complex has two quasi-degenerate locally-excited states of $A'$ and $A''$ symmetry, which correlate with the $B_{3u}$ and $B_{2u}$ excited singlets of the isolated Mg-porphyrin. The $A'$ state has a slightly lower excitation energy than the $A''$ state. The lowest CT state can be described almost exclusively as a single excitation from the highest occupied orbital of the Mg-porphyrin to the lowest unoccupied orbital of benzoquinone, and belongs to the $A'$ symmetry representation.

Equilibrium structures, vibrational normal modes and frequencies of porphyrin and the porphyrin cation in their ground electronic states have been determined in $D_{4h}$ symmetry, with density functional theory (DFT), using the hybrid B3LYP exchange-correlation functional,[32, 33] and the 6-311G(d,p) basis set. The minimum-energy structure of the ground state of Mg-porphyrin exhibits $D_{4h}$ symmetry, whereas its cation has a lower symmetry ($C_{4h}$). Indeed, both experiments and computations predict an in-plane distortion of the porphyrinic ring of the cation along an $a_{2g}$ mode ($a_g$ in the $C_{4h}$ group).[34–36] This distortion is caused by a pseudo Jahn-Teller (JT) interaction between the two lowest doublet states of the cation, labeled as $^2A_{2u}$ and $^2A_{1u}$ in the $D_{4h}$ group. Here we have assumed that only the lowest doublet state of the porphyrin cation,[34–36] *i.e.* the $^2A_{2u}$ state, is involved in the ET reaction, and the role of this pseudo-JT effect on the ET process has not been investigated. Geometries and vibrational modes of benzoquinone and of its anion have been computed in $D_{2h}$ symmetry at the CC2 level, using a cc-pVTZ basis set augmented with diffuse functions (aug-cc-pVTZ).[31] The DFT calculations have been performed using the Gaussian09 package,[37] and the CC2 calculations have been performed with the Turbomole software[38, 39]. The parameters of the Duschinsky transformations as well as linear and quadratic vibronic coupling parameters (*vide infra*) have been obtained using a modified version of the MolFC software.[40, 41]

### 2.3. *Determination of the parameters of the ET model*

The vibrational normal modes of benzoquinone and its anion, as well as those of the Mg-porphyrin in its first excited singlet state and its cation, are the basic elements of our model Hamiltonian. In the present model the equilibrium geometries and normal modes of Mg-porphyrin in the first excited state and in the ground state are assumed to be identical. This assumption is supported by the observation that in low-temperature electronic spectra of metalloporphyrins the 0-0 excitation of the $Q$ band carries a very large fraction of the total intensity.[42, 43] This approximation

allows us to strongly reduce the computational cost by avoiding the expensive calculation of the excited-state normal vibrations. Of course, only totally symmetric modes can give rise to linear vibronic couplings, whereas non-totally symmetric modes contribute to the Hamiltonian only through quadratic vibronic couplings, $\gamma_{ij}$.

Figure 2 shows the absolute values of the linear vibronic coupling constants $\kappa_i$. The full lines labeled with $\nu_1$ to $\nu_6$ are associated with the totally symmetric vibrations of benzoquinone depicted in figure 3. The dashed lines refer to the normal modes of Mg-porphyrin. Normal modes with frequencies higher than 2000 $\mathrm{cm}^{-1}$ have a very low vibronic activity and are not included in the figure (except $\nu_6$). It is seen that the modes associated with benzoquinone have a significantly stronger vibronic activity compared with those of Mg-porphyrin. This is also confirmed by the reorganization energies which amount to 3557 $\mathrm{cm}^{-1}$ for the reduction of benzoquinone ($\mathrm{Q}/\mathrm{Q}^-$) and to 771 $\mathrm{cm}^{-1}$ for the oxidation of Mg-porphyrin ($\mathrm{P}/\mathrm{P}^+$). The overall reorganization energy is 4328 $\mathrm{cm}^{-1}$, which is in good agreement with values obtained from the measurement of ET kinetics in cyclophane-bridged porphyrin-quinone systems.[44] We note that more than 80% of the total reorganization energy of the system can be ascribed to just five vibrational modes of benzoquinone (see figure 3), whose pronounced vibronic activity is caused by large changes of the benzoquinone geometry upon electron attachment. In particular, the computed geometries predict an elongation of the CO and CC bonds of about 0.06 and 0.04 $\mathring{\mathrm{A}}$, respectively, and a significant squeezing of the six-membered ring. The most active vibration of Mg-porphyrin corresponds to an in-plane distortion with a frequency of 1375 $\mathrm{cm}^{-1}$. The motion along this coordinate leads to a lowering of the $D_{4h}$ symmetry of the neutral Mg-porphyrin to the $C_{4h}$ symmetry of its cation. A CC stretching mode with a frequency of 1461 $\mathrm{cm}^{-1}$ is also particularly active.

A precise determination of the vertical energy difference $\Delta E_v$ is a challenging task, which would require also a consideration of environmental effects. Therefore, we consider $\Delta E_v$ as a parameter in this work and explore the energy range $[-0.25, 0.25]$ eV, which amounts to the modeling of an ET reaction with a driving force in the range $0.3 - 0.8$ eV. This choice is motivated by the fact that similar values have been reported in porphyrin-quinone type complexes.[2, 44]

Finally, the diabatic coupling, $V$, between the excited state, $\left|\mathrm{P}^*\mathrm{Q}\right\rangle$, and the CT state, $\left|\mathrm{P}^+\mathrm{Q}^-\right\rangle$, is computed by the *ab initio* diabatization procedure explained in Sec. 2.2, which gives a value of 120 $\mathrm{cm}^{-1}$ at the CASSCF level. Empirical estimates

based on Marcus theory of ET in metallo-porphyrin-quinone systems with a similar edge-to-edge distance suggest values between 100-160 $\mathrm{cm}^{-1}$, and similar values can be obtained using Hopfield's semiempirical formula.[45]

### 2.4. *Multilayer multiconfiguration time-dependent Hartree theory*

To simulate the quantum dynamics of the ET system, we use the multilayer (ML) formulation [46] of the multiconfiguration time-dependent Hartree (MCTDH) method [47–51]. The method as well as applications to different reactions have been described in detail previously [46, 52–54]. Here, we only briefly introduce the general idea and give some details specific to the application in this work.

The ML-MCTDH theory[46] is a rigorous variational method to propagate wave packets in systems with many degrees of freedom. In this approach, the wave function is represented by a recursive, layered expansion,

$$|\Psi(t)\rangle = \sum_{j_1}\sum_{j_2}\dots\sum_{j_p} A_{j_1 j_2 \dots j_p}(t) \prod_{\kappa=1}^{p} |\varphi_{j_\kappa}^{(\kappa)}(t)\rangle, \tag{9a}$$

$$|\varphi_{j_\kappa}^{(\kappa)}(t)\rangle = \sum_{i_1}\sum_{i_2}\dots\sum_{i_{Q(\kappa)}} B^{\kappa,j_\kappa}_{i_1 i_2 \dots i_{Q(\kappa)}}(t) \prod_{q=1}^{Q(\kappa)} |v_{i_q}^{(\kappa,q)}(t)\rangle, \tag{9b}$$

$$|v_{i_q}^{(\kappa,q)}(t)\rangle = \sum_{\alpha_1}\sum_{\alpha_2}\dots\sum_{\alpha_{M(\kappa,q)}} C^{\kappa,q,i_q}_{\alpha_1 \alpha_2 \dots \alpha_{M(\kappa,q)}}(t) \prod_{\gamma=1}^{M(\kappa,q)} |\xi^{\kappa,q,\gamma}_{\alpha_\gamma}(t)\rangle, \tag{9c}$$

...

where $A_{j_1 j_2 \dots j_p}(t)$, $B^{\kappa,j_\kappa}_{i_1 i_2 \dots i_{Q(\kappa)}}(t)$, $C^{\kappa,q,i_q}_{\alpha_1 \alpha_2 \dots \alpha_{M(\kappa,q)}}(t)$ etc. are the expansion coefficients for the first, second, third layers etc., respectively; $|\varphi_{j_\kappa}^{(\kappa)}(t)\rangle$, $|v_{i_q}^{(\kappa,q)}(t)\rangle$, $|\xi^{\kappa,q,\gamma}_{\alpha_\gamma}(t)\rangle$ etc. are the single particle functions (SPF) for the first, second, third layers etc., respectively. The notations beyond the first layer are as follows. In Eq. (9b), $Q(\kappa)$ is the number of (level 2) single particle (SP) groups for the second layer that belong to the $\kappa$th (level 1) SP group in the first layer, i.e., there are a total of $\sum_{\kappa=1}^{p} Q(\kappa)$ second layer SP groups. Continuing along the multilayer hierarchy, $M(\kappa, q)$ in Eq. (9c) is the number of (level 3) SP groups for the third layer that belong to the $q$th (level 2) SP group of the second layer and the $\kappa$th (level 1) SP group of the first layer, resulting in a total of $\sum_{\kappa=1}^{p}\sum_{q=1}^{Q(\kappa)} M(\kappa, q)$ third-layer

SP groups. Such a recursive expansion can be carried out to an arbitrary number of layers. To terminate the multilayer hierarchy at a particular level, the SPFs in the deepest layer are expanded in terms of time-independent configurations. For example, in the four-layer version of the ML-MCTDH theory, the fourth layer is expanded in the time-independent basis functions/configurations, each of which may still contain several Cartesian degrees of freedom. In the calculation considered below up to three dynamical layers are employed.

Applying the Dirac-Frenkel variational principle, the ML-MCTDH equations of motion can be derived as a set of coupled, nonlinear differential equations for the expansion coefficients of all the layers.[46, 54] The implementation is somewhat tedious, but nevertheless straightforward. The inclusion of several dynamically optimized layers in the ML-MCTDH method provides more flexibility in the variational functional, which significantly advances the capabilities of performing wavepacket propagations in complex systems. The number of degrees of freedom that the ML-MCTDH theory can handle grows exponentially with the number of dynamically contracted layers, provided that the overall strength of the correlation between the degrees of freedom remains similar. This has been demonstrated by several applications to quantum dynamics in large molecular systems and in the condensed phase including many degrees of freedom [46, 52, 53, 55, 55–61]. Manthe recently has introduced an even more flexible formulation based on a layered correlation-discrete-variable representation (CDVR).[62–64]

## 3. Results and Discussion

The methodology outlined above has been applied to simulate the dynamics of the ET reaction in the Mg-porphyrin-benzoquinone complex. To analyze the ET mechanism, in particular the role of the vibrational degrees of freedom, we have considered models of increasing complexity, ranging from models which only include a selected number of vibrational modes to a model including all intramolecular vibrational modes. As the observable characterizing the ET dynamics, we consider the population of the initially excited diabatic donor state $\left|\mathrm{P^*Q}\right\rangle$. Neglecting temperature effects, the population is given by

$$P(t) = \mathrm{tr}|\mathrm{P^*Q}\rangle\langle\mathrm{P^*Q}|e^{-iHt}|\mathrm{P^*Q}\rangle|\mathbf{0}\rangle\langle\mathbf{0}|\langle\mathrm{P^*Q}|e^{iHt} \tag{10}$$

where the trace is over all electronic and vibrational degrees of freedom and $|\mathbf{0}\rangle$ denotes the vibrational ground state in the ground electronic state $|\mathrm{PQ}\rangle$.

### 3.1. *ET dynamics including the totally symmetric modes of benzoquinone*

Since more than 80% of the reorganization energy arises from the totally symmetric vibrations of benzoquinone, a reduced-dimensionality model including only these six modes should already provide relevant information on the microscopic mechanisms which control the ET dynamics. In figure 4, the population, $P(t)$, of the initially photoexcited electronic state $\left|\mathrm{P^*Q}\right\rangle$ is depicted for several values of the vertical energy gap $\Delta E_v$, in the range $[-2000,2000]$ cm$^{-1}$. The oscillations of the electronic population with time are a clear indication that the dynamics is dominated by resonances between a few vibronic states. This is also confirmed by the drastic changes which are observed upon small variations of the energy gap. Indeed, for $\Delta E_v = 0$ the population transfer is almost complete after about 300 fs, while for $\Delta E_v = \pm 800$ cm$^{-1}$ the maximum population transfer observed is only about 40%. This behavior is the result of the reduced number of degrees of freedom included in the model, which provide only a few vibronic states effectively involved in the electron transfer, not allowing for a completely irreversible ET process. The 'kink'-type structures observed in the electronic populations in figure 4 are not due to limited time resolution or numerical errors, but are the result of the vibronic dynamics in a system with a low density of states.

### 3.2. *ET dynamics including all totally symmetric modes*

The transition to a fully irreversible regime becomes manifest when more degrees of freedom are included in the dynamical model. Figures 5 and 6 show the population of the initial photoexcited electronic state $\left|\mathrm{P^*Q}\right\rangle$ for several values of the vertical energy gap $\Delta E_v$, when all totally symmetric vibrations of the complex (*i.e.* 23 vibrational modes) are included in the dynamics. Again, temperature effects are neglected, *i.e.* the system is assumed to be in its vibrational ground state prior to optical excitation. A comparison with the results of figure 4 shows that the electronic population decay curves become significantly smoother upon inclusion of a larger number of degrees of freedom, and, in particular, the oscillations disappear completely on the timescale studied. For a barrierless process (*i.e.* $\Delta E_v = 0$), $P(t)$ exhibits an almost exactly exponential decay with a decay constant of 2.7 ps$^{-1}$.

For negative values of $\Delta E_v$ (figure 6), *i.e.* increasing the driving force, the ET rate slows down, reaching 1.9 $ps^{-1}$ for $\Delta E_v = -2000$ $cm^{-1}$. On the other hand, for positive values of $\Delta E_v$ (figure 5), *i.e.* reducing the driving force, an increase of the ET rate is observed with a maximum kinetic constant of 4.9 $ps^{-1}$ at $\Delta E_v = 1600$ $cm^{-1}$. Further increasing $\Delta E_v$ to 2000 $cm^{-1}$, which correspond to a driving force of about 2400 $cm^{-1}$, leads to a significant lowering of the ET rate.

The above results cannot be described in terms of classical ET rate theory, which predicts a maximum rate for the barrierless process, which reveals that quantum effects play a major role. Indeed, for $\Delta E_v >> 0$ the number of vibronic states which are effectively coupled to the initially photoexcited state becomes so small that the dynamics is controlled by a few resonances, and the classical description of ET is not valid. On the other hand, for $\Delta E_v << 0$ the density of final states coupled with the initially photoexcited state becomes a quasi-continuum and the classical interpretation of ET rates applies. Models with $\Delta E_v << 0$ correspond to the inverted regime, where a decrease of the ET rate with increasing $\Delta E_v$ is expected.

To analyze the ET mechanism and rationalize the above results, dynamical simulations using the simplified spin-boson-type (SB) model (derived from the model Hamiltonian of equation (1) by neglecting both Duschinsky effects and changes in the vibrational frequencies), have been performed. The results are shown in figure 7. As in the previous case, for $\Delta E_v = 0$ the electronic population follows very closely a single-exponential decay with a constant of 3.5 $ps^{-1}$. In the same way, larger driving forces ($\Delta E_v < 0$) lead to a lowering of the ET rate. For smaller driving forces ($\Delta E_v > 0$), the electronic population shows a fast decay on the short timescale, followed by oscillations at longer times. Such a behavior is typical for spin-boson dynamics, in which the electronic coherences are quenched by the slower nuclear motion. Our results suggest, that, although the full-Hessian model does not exhibit the coherent oscillations observed in the SB model, their overall ET dynamics follow a similar pattern. The role of the change of the vibrational frequencies and of Duschinsky effects is thus to provide a more effective vibrational dephasing mechanism, resulting in an incoherent dynamics for all values of $\Delta E_v$. So far, only a very limited number of studies have investigated the role of second-order vibronic couplings on ET rates, mostly for model systems, and in some cases an increase in the ET rate has been reported.[65, 66] Recent applications of radiationless transition theory to ET processes in realistic systems have shown that the inclusion

of Duschinsky effects can have a strong impact on the Franck-Condon-weighted density of states, which controls the ET rate.[21] The present accurate quantum dynamical study employing the ML-MCTDH method confirms and extends these findings beyond the assumptions of rate theory.

### 3.3. *ET dynamics including all vibrational modes*

Using the ML-MCTDH methodology, it is possible to perform simulations of the electron-transfer dynamics including all 135 intramolecular vibrational degrees of freedom of the complex. Due to the significant computational cost of these calculations, we have performed simulations for a shorter time interval of 400 fs for $\Delta E_v = 0, \pm 800, \pm 1200, \pm 2000$ cm$^{-1}$. The ET dynamics as represented by the population of the donor state is reported in figures 8 and 9. The results of the complete model exhibit similar qualitative trends as the lower dimensionality model discussed above. Indeed, for $\Delta E_v << 0$, the population of the initial electronic state follows an exponential decay and the ET rate decreases with increasing driving force. Increasing $\Delta E_v$ up to 1200 cm$^{-1}$, the ET dynamics shows only small variations. However, going from 1200 to 2000 cm$^{-1}$ a significant change of the population dynamics is observed. As already pointed out above, this behavior can be explained considering that for $\Delta E_v = 2000$ cm$^{-1}$ only a small number of vibronic states become effectively involved in the ET process and the classical rate analysis does not hold. It is interesting to note that second-order vibrational terms in the Hamiltonian, arising from the non-totally symmetric modes of the system, significantly modify the ET dynamics. Indeed, as can be seen from figure 10 for $\Delta E_v = 0$, the population decay in the dynamics including all vibrational modes is faster than the population decay of the model including only the totally symmetric modes. On the other hand, the two decay rates in figure 10 are essentially the same for the first 100 fs. These results demonstrate that second-order expansion terms of the potential-energy surfaces arising from non-totally symmetric modes can have a strong impact on the ET dynamics and should be included in models describing this type of ET reactions.

## 4. Conclusions

We have studied the photoinduced ET dynamics in the donor-acceptor complex Mg-porphyrin-benzoquinone, employing a microscopic model based on *ab initio*

electronic-structure calculations. The quantum dynamics has been treated with the ML-MCTDH method, which allows an accurate description of the dynamics of the problem including all vibrational degrees of freedom. These results extend our previous work for lower-dimensionality models.[17]

The analysis of models of increasing complexity and dimensionality shows that most of the vibronic activity during the ET reaction is associated with the nuclear motion in the benzoquinone moiety, mainly due to large changes of its molecular geometry upon electron attachment. The computed intramolecular reorganization energy of the complex of about 4328 $cm^{-1}$ is in good agreement with experimental estimates for similar systems. The quantum dynamical simulations demonstrate the important role of vibronic resonances, which give rise to a non-classical behavior of ET rates. Totally symmetric vibrations of the redox pair are able to drive the ET process by providing an efficient mechanism of energy transfer between the electronic and nuclear degrees of freedom. Non-totally symmetric vibrations affect the ET dynamics by providing new channels for the electronic transition, thus increasing the overall ET rate.

Our results also show that Duschinsky effects can have a significant impact on the overall ET process. Therefore, the application of the spin-boson model to describe ET in donor-acceptor complexes has to be considered with caution, in particular if the dynamics is dominated by intramolecular modes, as in the system considered in this work. On the other hand, the determination of model potential-energy surfaces including Duschinsky effects can be computationally very demanding for large systems of chemical interest.

The present work opens the way for several extensions. Particularly interesting will be the study of ET reactions coupled to water oxidation processes as proposed, e.g. by Sobolewski and Domcke[18], which will be the subject of future research.

## Acknowledgments

This work is dedicated to Bill Miller on the occasion of his 70th birthday. MT and HW are deeply indebted to Bill Miller for many insightful discussions on quantum and semiclassical dynamics. This work has been supported by the Deutsche Forschungsgemeinschaft through a research grant (MT), the National Science Foundation CHE-1012479 (HW), and the cluster of excellence 'Munich Center for Advanced Photonics' (WD and MT) and has used resources of the computing centers

in Munich (LRZ) and Jülich (JSC), which is gratefully acknowledged.

## References

[1] B. O'Regan and M. Grätzel, Nature **353** (6346), 737 (1991).

[2] M.R. Wasielewski, Chem. Rev. **92** (3), 435 (1992).

[3] A. Nitzan, *Chemical Dynamics in Condensed Phases: Relaxation, Transfer, and Reactions in Condensed Molecular Systems* (Oxford University Press, USA, Oxford, 2006).

[4] V. May and O. Kühn, *Charge and Energy Transfer Dynamics in Molecular Systems* (Wiley-VCH, Weinheim, 2004).

[5] A.J. Leggett, S. Chakravarty, A.T. Dorsey, M.P. Fisher and W. Zwerger, Rev. Mod. Phys. **59**, 1 (1987).

[6] A. Warshel and W.W. Parson, Quarterly Reviews of Biophysics **34** (04), 563 (2001).

[7] U. Weiss, *Quantum Dissipative Systems*, 2nd ed. (World Scientific, Singapore, 1999).

[8] R. Egger and C.H. Mak, Phys. Rev. B **50**, 15210 (1994).

[9] N. Makri and D.E. Makarov, J. Chem. Phys. **102**, 4611 (1995).

[10] H. Wang, M. Thoss and W.H. Miller, J. Chem. Phys. **115**, 2979 (2001).

[11] M. Thoss, H. Wang and W.H. Miller, J. Chem. Phys. **114**, 9220 (2001).

[12] L. Mühlbacher and R. Egger, J. Chem. Phys. **118**, 179 (2003).

[13] R. Bulla, N. Tong and M. Voitja, Phys. Rev. Lett. **91**, 170601 (2003).

[14] F. Anders, R. Bulla and M. Voitja, Phys. Rev. Lett. **98**, 210402 (2007).

[15] Y. Zhou and J. Shao, J. Chem. Phys. **128**, 034106 (2008).

[16] H. Wang and M. Thoss, New J. Phys. **10**, 115005 (2008).

[17] R. Borrelli and W. Domcke, Chem Phys. Lett. **498** (Raf), 230 (2010).

[18] A.L. Sobolewski and W. Domcke, J. Phys. Chem. A **112** (32), 7311 (2008).

[19] R. Borrelli, M. Di Donato and A. Peluso, Biophys. J. **89**, 830 (2005).

[20] R. Borrelli, M. Di Donato and A. Peluso, Theor. Chem. Acc. **117**, 957 (2007).

[21] R. Borrelli and A. Peluso, Phys. Chem. Chem. Phys. **13** (10), 4420 (2011).

[22] W.W. Parson and A. Warshel, J. Phys. Chem. B **108** (29), 10474 (2004).

[23] M. Thoss, I. Kondov and H. Wang, Phys. Rev. B **76**, 153313 (2007).

[24] M. Thoss, I. Kondov and H. Wang, Chem. Phys. **304**, 169 (2004).

[25] I. Kondov, M. Thoss and H. Wang, J. Phys. Chem. A **110**, 1364 (2006).

[26] W. Domcke and G. Stock, Theory of ultrafast nonadiabatic excited-state processes and their spectroscopic detection in real time, in *Adv. Chem. Phys.*, Vol. 100, p. 1.

[27] J.E. Subotnik, J. Vura-Weis, A.J. Sodt and M.A. Ratner, J. Phys. Chem. A **114** (33), 8665 (2010).

[28] D. Simah, B. Hartke and H. Werner, J. Chem. Phys. **111** (10), 4523 (1999).

[29] W. Domcke, C. Woywod and M. Stengle, Chem. Phys. Lett. **226** (3-4), 257 (1994).

[30] H.J. Werner, P.J. Knowles, R. Lindh, F.R. Manby, M. Schütz *et al.*, MOLPRO, version 2008.2, a package of ab initio programs Cardiff, UK, 2008, see http://www.molpro.net.

[31] T.H. Dunning, J. Chem. Phys. **55**, 716 (1971).

[32] A.D. Becke, Phys. Rev. A **38**, 3098 (1988).

[33] C. Lee, W. Yang and R.G. Parr, Phys. Rev. B **37**, 785 (1988).

[34] R.S. Czernuszewicz, K.A. Macor, X.Y. Li, J.R. Kincaid and T.G. Spiro, J. Am. Chem. Soc. **111** (11), 3860 (1989).

[35] K. Prendergast and T.G. Spiro, J. Phys. Chem. **95** (24), 9728 (1991).

[36] T. Vangberg, R. Lie and A. Ghosh, J. Am. Chem. Soc. **124** (27), 8122 (2002).

[37] M.J. Frisch, G.W. Trucks, H.B. Schlegel, G.E. Scuseria and M.A.R. *et al.*, Gaussian 09 Revision A.1 Gaussian Inc. Wallingford CT 2009.

[38] TURBOMOLE V6.1 2009, University of Karlsruhe and Forschungszentrum Karlsruhe GmbH, available at `http://www.turbomole.com`. .

[39] C. Hättig, J. Chem. Phys. **118** (17), 7751 (2003).

[40] R. Borrelli and A. Peluso, MolFC: A program for Franck-Condon integrals calculation Package available online at `http://www.theochem.unisa.it`.

[41] R. Borrelli and A. Peluso, J. Chem. Phys. **119**, 8437 (2003).

[42] L. Edwards, D.H. Dolphin, M. Gouterman and A.D. Adler, J. Mol. Spectrosc. **38**, 16 (1971).

[43] A. Starukhin, A. Shulga and J. Waluk, Chem. Phys. Lett. **272** (5-6), 405 (1997).

[44] T. Haberle, J. Hirsch, F. Pollinger, H. Heitele, M.E. Michel-Beyerle, C. Anders, A. Dohling, C. Krieger, A. Ruckemann and H.A. Staab, J. Phys. Chem. **100** (46), 18269 (1996).

[45] J.J. Hopfield, Proc. Natl. Acad. Sci. USA **71**, 3640 (1974).

[46] H. Wang and M. Thoss, J. Chem. Phys. **119**, 1289 (2003).

[47] H.D. Meyer, U. Manthe and L. Cederbaum, Chem. Phys. Lett. **165**, 73 (1990).

[48] U. Manthe, H.D. Meyer and L.S. Cederbaum, J. Chem. Phys. **97**, 3199 (1992).

[49] M.H. Beck, A. Jäckle, G.A. Worth and H.D. Meyer, Phys. Rep. **324**, 1 (2000).

[50] H.D. Meyer and G.A. Worth, Theor. Chem. Acc. **109**, 251 (2003).

[51] H.D. Meyer, F. Gatti and G. Worth, *Multidimensional Quantum Dynamics: MCTDH Theory and Applications* (Whiley-VCH, Weinheim, 2009).

[52] M. Thoss, I. Kondov and H. Wang, Chem. Phys. **304**, 169 (2004).

[53] M. Thoss and H. Wang, Chem. Phys. **322**, 210 (2006).

[54] H. Wang and M. Thoss, J. Chem. Phys. **131**, 024114 (2009).

[55] H. Wang and M. Thoss, Chem. Phys. Lett. **389**, 43 (2004).

[56] M. Thoss, W. Domcke and H. Wang, Chem. Phys. **296**, 217 (2004).

[57] H.Y. Wang, S. Lin and N.W. Woodbury, J. Phys. Chem. B **110**, 6956 (2006).

[58] I. Kondov, M. Cizek, C. Benesch, H. Wang and M. Thoss, J. Phys. Chem. C **111**, 11970 (2007).

[59] I.R. Craig, H. Wang and M. Thoss, J. Chem. Phys. **127**, 144503 (2007).

[60] J. Li, I. Kondov, H. Wang and M. Thoss, J. Phys. Chem. C **114**, 18481 (2010).

[61] O. Vendrell and H.D. Meyer, J. Chem. Phys. **134**, 2011 (044135).

[62] U. Manthe, J. Chem. Phys. **128**, 164116 (2008).

[63] U. Manthe, J. Chem. Phys. **130**, 054109 (2009).

[64] T. Westermann, R. Brodbeck, A. Rozhenko and W.S. and, J. Chem. Phys. **135**, 184102 (2011).

[65] G. Sando, K. Spears, J. Hupp and P. Ruhoff, J. Phys. Chem. A **105**, 5317 (2001).

[66] K.A. Velizhanin and H. Wang, J. Chem. Phys. **131** (9), 094109 (2009).

Figure 1. Structure of the Mg-porphyrin-benzoquinone donor-acceptor pair as used in the electronic-structure calculations. The complex has $C_s$ symmetry.

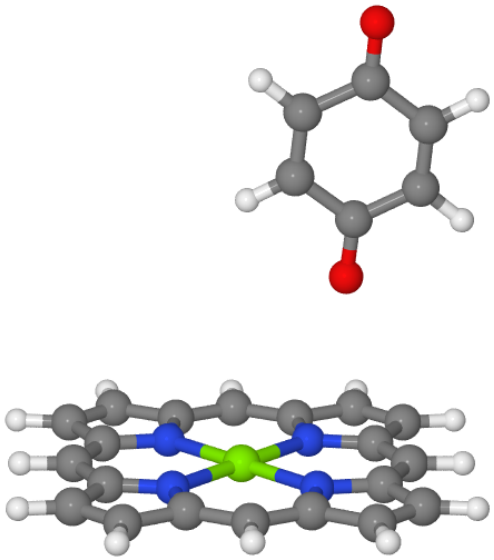

Figure 2. Linear electronic-vibrational coupling constants $\kappa_i$ for the totally symmetric normal modes of benzoquinone (full lines) and Mg-porphyrin (dashed lines).

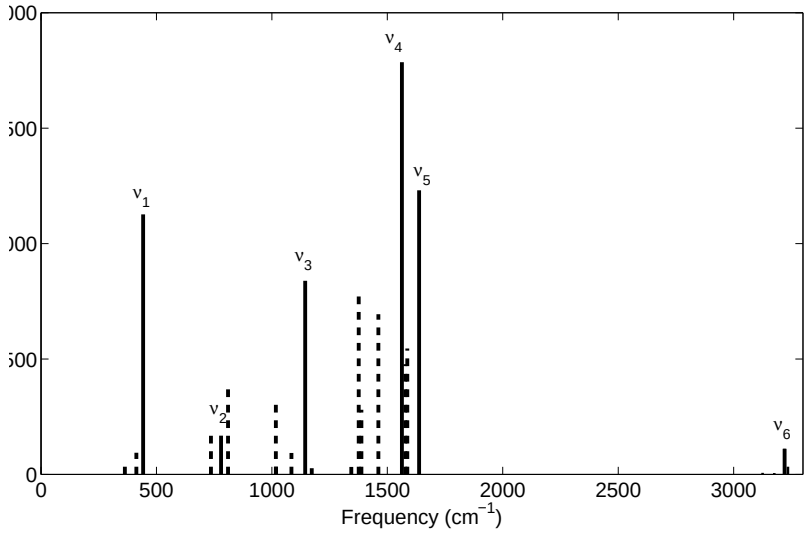

Figure 3. Totally symmetric normal vibrations of neutral benzoquinone and their vibrational frequencies (in $cm^{-1}$), computed at the CC2 level with the aug-cc-pVTZ basis set. The vibrational frequencies of the corresponding modes of the benzonquinone anion are given in parentheses.

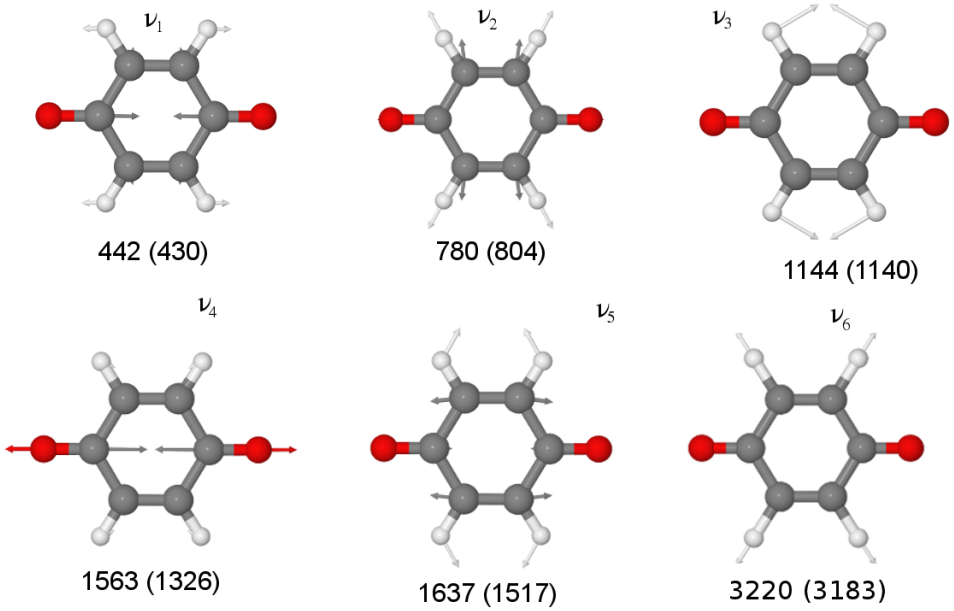

Figure 4. Population of the donor electronic state obtained including only the six totally symmetric modes of benzoquinone, for different values of the energy gap $\Delta E_v$.

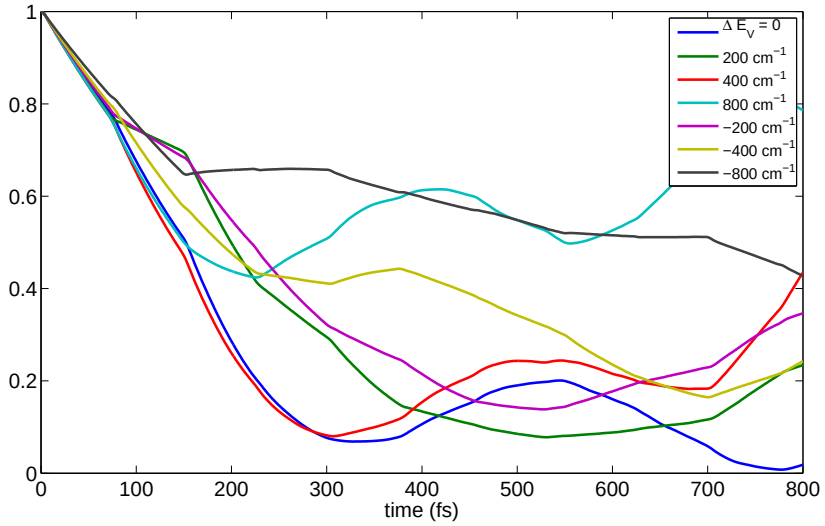

Figure 5. Electronic population dynamics of the ET process obtained including all 23 totally symmetric modes of the complex, for different values of the energy gap $\Delta E_v$, $\Delta E_v > 0$. The curves represent the probability of finding the system in the initial locally-excited electronic state at time $t$.

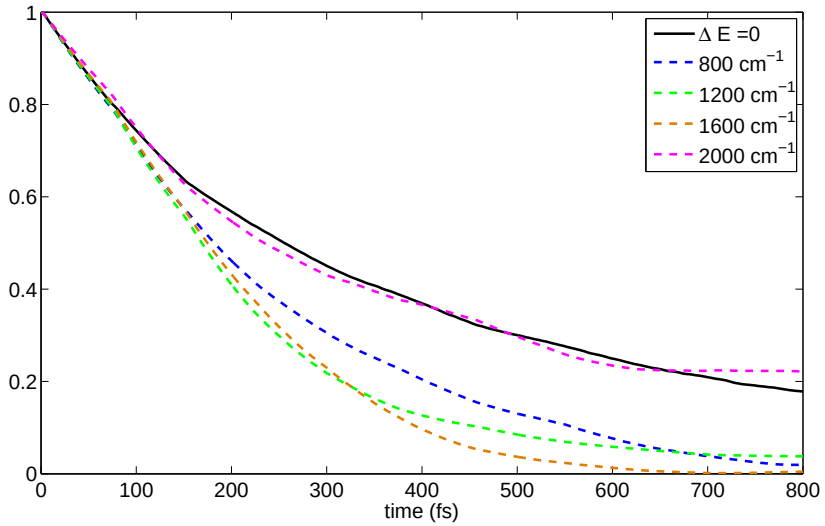

Figure 6. Electronic population dynamics of the ET process obtained including all 23 totally symmetric modes of the complex, for different values of the energy gap $\Delta E_v$, $\Delta E_v < 0$. The curves represent the population of the initially excited donor state at time $t$.

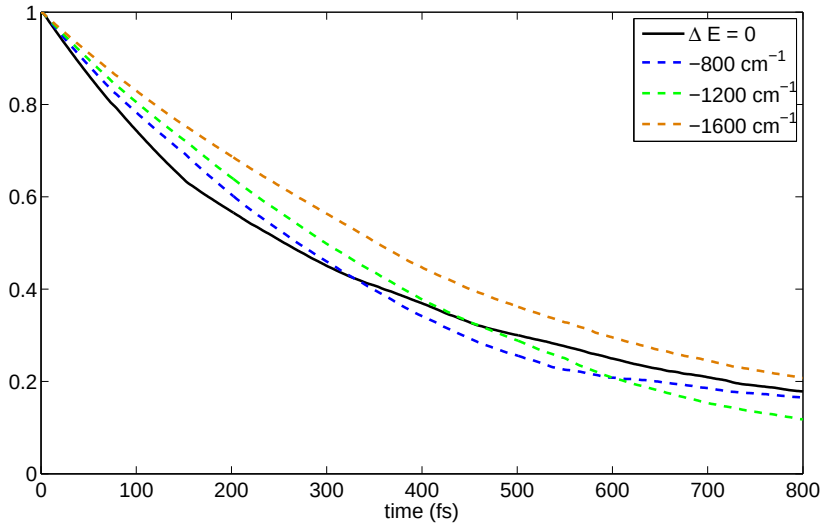


Figure 7. Electronic population dynamics of the ET process, obtained using a spin-boson model. All 23 totally symmetric modes of the complex are included. The curves represent the population of the initially excited donor state at time $t$, for different values of the energy gap $\Delta E_v$.

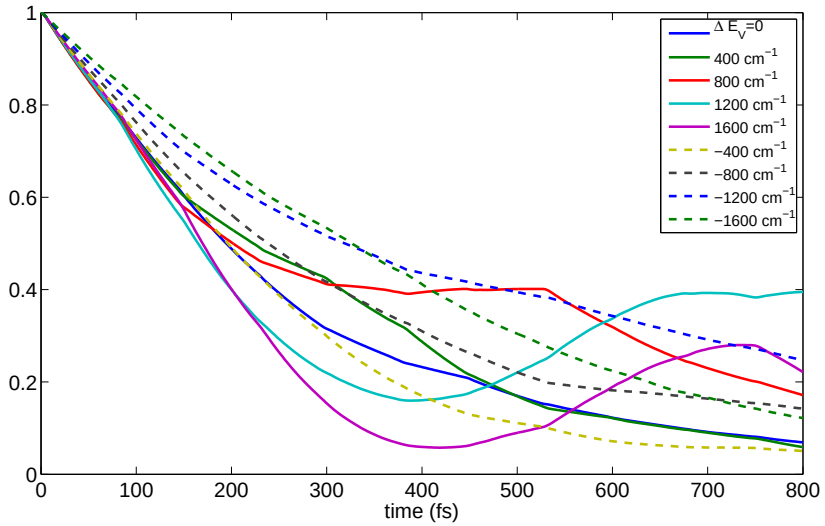

Figure 8. Electronic population dynamics of the ET process, obtained including all 135 intramolecular nuclear degrees of freedom of the complex, for positive values of the energy gap $\Delta E_v$. The curves represent the population of the initially excited donor state at time $t$.

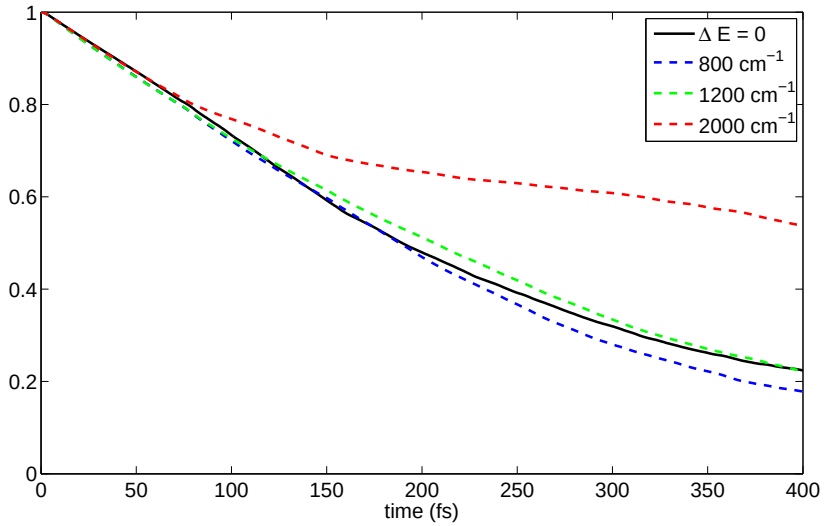

Figure 9. Electronic population dynamics of the ET process, obtained including all 135 intramolecular nuclear degrees of freedom of the complex, for negative values of the energy gap, $\Delta E_v$. The curves represent the population of the initially excited donor state at time $t$.

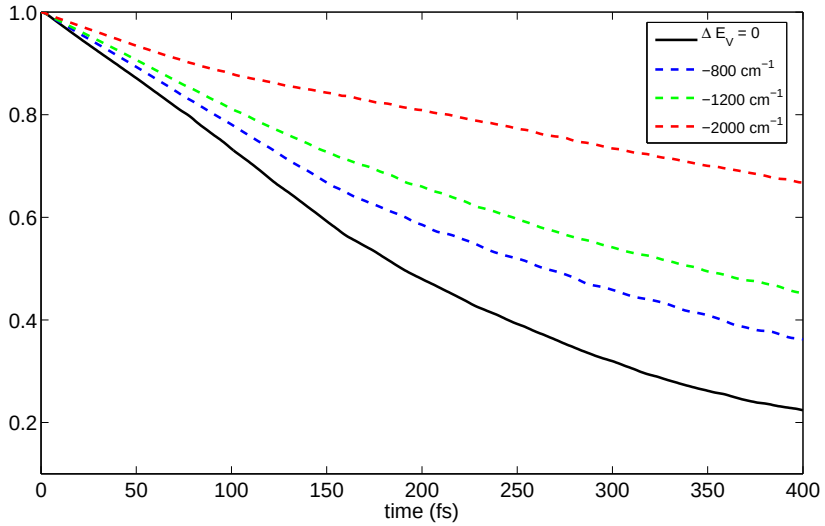

Figure 10. Electronic population dynamics of the ET process, obtained including all modes (- - -) or only the totally symmetric modes (—), respectively, for $\Delta E_v = 0$. The curves represent the population of the initially excited donor state at time $t$.